

Kent Academic Repository

Full text document (pdf)

Citation for published version

Erdelyi, Ralph-Alexandru and Duma, Virgil-Florin and Sinescu, Cosmin and Dobre, George Mihai and Bradu, Adrian and Podoleanu, Adrian G.H. (2020) Dental Diagnosis and Treatment Assessments: Between X-rays Radiography and Optical Coherence Tomography. *Materials*, 13 (21). p. 4825. ISSN 1996-1944.

DOI

<https://doi.org/10.3390/ma13214825>

Link to record in KAR

<https://kar.kent.ac.uk/83857/>

Document Version

Author's Accepted Manuscript

Copyright & reuse

Content in the Kent Academic Repository is made available for research purposes. Unless otherwise stated all content is protected by copyright and in the absence of an open licence (eg Creative Commons), permissions for further reuse of content should be sought from the publisher, author or other copyright holder.

Versions of research

The version in the Kent Academic Repository may differ from the final published version.

Users are advised to check <http://kar.kent.ac.uk> for the status of the paper. **Users should always cite the published version of record.**

Enquiries

For any further enquiries regarding the licence status of this document, please contact:

researchsupport@kent.ac.uk

If you believe this document infringes copyright then please contact the KAR admin team with the take-down information provided at <http://kar.kent.ac.uk/contact.html>

1 Article

2 **Dental Diagnosis and Treatment Assessments:** 3 **Between X-rays Radiography and Optical Coherence** 4 **Tomography**

5 **Ralph-Alexandru Erdelyi** ^{1,2}, **Virgil-Florin Duma** ^{2,1,3*}, **Cosmin Sinescu** ³, **George Mihai Dobre** ⁴,
6 **Adrian Bradu** ⁴, and **Adrian Podoleanu** ⁴

7 ¹ Doctoral School, Polytechnic University of Timisoara, 1 Mihai Viteazu Ave., 300222 Timisoara, Romania;
8 ralph.erdelyi@student.upt.ro (R.-A.E.)

9 ² 3OM Optomechatronics Group, “Aurel Vlaicu” University of Arad, 77 Revolutiei Ave., 310130 Arad,
10 Romania;

11 ³ Research Center in Dental Medicine using Conventional and Alternative Technologies, School of Dental
12 Medicine, “Victor Babes” University of Medicine and Pharmacy of Timisoara, 9 Revolutiei 1989 Ave.,
13 300070 Timisoara, Romania; minosinescu@gmail.com (C.M.);

14 ⁴ Applied Optics Group, School of Physics, University of Kent, Canterbury, United Kingdom, CT2 7NR;
15 gd@kent.ac.uk (G.D.); a.bradu@kent.ac.uk (A.B.); a.g.h.podoleanu@kent.ac.uk (A.P.)

16 * Correspondence: duma.virgil@osamember.org; Tel.: +40-751-511451 (V.-F.D.)

17 Received: date; Accepted: date; Published: date

18 **Abstract:** A correct diagnosis in dental medicine is typically provided only after clinical and
19 radiological evaluations. They are also required for treatment assessments. The aim of this study is
20 to establish the boundaries from which a modern, although established imaging technique, Optical
21 Coherence Tomography (OCT) is more suitable than the common X-ray radiography to assess
22 dental issues and treatments. The most common methods for daily-basis clinical imaging are
23 utilized in this study for extracted teeth (but also for other dental samples and materials), i.e.,
24 panoramic, intraoral radiography and three-dimensional (3D) cone beam computed tomography
25 (CBCT). Advantages of using OCT as an imaging method in dentistry are discussed, with a focus
26 on its superior image resolution. Drawbacks related to its limited penetration depth and Field-of-
27 View (FOV) are pointed out. High-quality radiological investigations are performed, measurements
28 are done, and data collected. The same teeth and samples are also imaged (mostly) with an in-house
29 developed Swept Source (SS)-OCT system, Master-Slave enhanced. Some of the OCT investigations
30 employed two other in-house developed OCT systems, Spectral Domain (SD) and Time Domain
31 (TD). Dedicated toolbars from Romexis software (Planmeca, Helsinki, Finland) are used to perform
32 measurements using both radiography and OCT. Clinical conclusions are drawn from the
33 investigations. Upsides and downsides of the two medical imaging techniques are concluded for
34 each type of considered diagnosis. For treatment assessments, it is concluded that OCT is more
35 appropriate than radiography in all applications, except bone-related investigations and
36 periodontitis that demand data from higher-penetration depths than possible with the current level
37 of OCT technology.

38 **Keywords:** Biomedical imaging; dental medicine; X-ray radiography; Optical Coherence
39 Tomography (OCT); Cone Beam Computed Tomography (CBCT); dental cavities; biocompatible
40 materials; optical measurements; quantitative assessments.

41 **1. Introduction**

42 Dentistry has been evolving fast in the last decades through technological advances in both
43 diagnosis and treatment [1-3]. For diagnosis there are several types of medical imaging techniques

44 available, including X-ray radiography, laser-based pens for the detection of cavities, as well as
45 Optical Coherence Tomography (OCT) [4-7].

46 The most common methods for daily-basis clinical imaging in dental medicine are intraoral and
47 panoramic radiography, as well as three-dimensional (3D) Cone Beam Computed Tomography
48 (CBCT). One of their drawbacks is the patients' concern with being exposed to X-ray radiation, which
49 is ionizing and harmful for living tissue. In this respect, the radiation dose must be properly
50 calculated by technical personnel for every method [8], while X-ray units and investigations must be
51 improved to reduce the radiation dose [9]. This is ideally achieved without losing imaging
52 performances, as accurate high-quality images with high resolution, good contrast and no artefacts
53 are mandatory to correctly diagnose a patient or to assess a performed treatment. Nowadays digital
54 X-ray units (equipped with appropriate sensors and dedicated software) can be optimized to
55 enhance, process, and analyze in-depth obtained images. X-rays techniques are limited in resolution:
56 around 127 μm for panoramic, 144 μm for intraoral radiographies and 75 μm for CBCT [9]. Some
57 dental issues cannot thus be correctly assessed whatever the type of radiography nor using visual
58 observation. In consequence, other medical imaging techniques are necessary for clinicians to allow
59 them to provide a quality treatment.

60 OCT is such an imaging technique that can be utilized to diagnose dental affections [10-17] and
61 to assess performed treatments [14]. OCT is not yet a common imaging method in dentistry, although
62 it has imposed itself in ophthalmoscopy [4, 18], but also for skin investigations [19] (in conjunction
63 with confocal microscopy) and endoscopy [20,21]. As OCT is using low-power IR laser radiation, it
64 is entirely non-invasive, with the advantage of avoiding patients' exposure to radiation-in contrast to
65 X-ray techniques. However, image resolution in OCT is much better, with common values of 8 μm
66 for the axial resolution reported in the current manuscript and values of 2 μm (both axial and lateral)
67 as state-of-the-art [22], while sub-micrometer values have also been explored (but in VIS, not in IR,
68 therefore not applicable in dentistry, as the penetration depth would be too small) [23]. While the
69 possible utility of OCT for different Dental Medicine investigations has been demonstrated by
70 numerous studies, to our knowledge a study on establishing clear suitability of this technique versus
71 X-rays considering the existing range of dental issues and applications is still necessary.

72 The aim of this work is to contribute in this direction, to establish which conditions affecting
73 hard tissue in the oral cavity can be investigated only with X-rays, with both X-rays and OCT, as well
74 as only with OCT. Advantages and drawbacks of each technique must also be considered. Comparing
75 OCT with (common) radiography, its clear drawback is the much lower penetration depth. This is
76 inversely proportional to the density of the material being investigated, therefore limited to at most
77 1.5 mm for hard dental tissue or bone. On the other hand, OCT images reveal dental issues at an
78 earlier stage than radiographs due to their superior resolution [17].

79 Quantitative assessment is another important rationale for such a comparative study.
80 Measurements with dedicated software can be used to serve investigation of cavities, secondary
81 cavities, length of the root canal, or periodontitis. Without quantitative tools, images delivered by
82 any technique can only serve qualitative analysis. Thus, the image of a cavity, for example (as
83 delivered by OCT), must be processed and analyzed to provide a quantitative information [24]. To
84 compare X-rays techniques and OCT from the point of view of the precision of such assessments is
85 another aim of this work. To fulfill its scope, a range of *in vivo* investigated clinical cases in the oral
86 cavity and *ex vivo* assessments (the latter on extracted teeth) are considered in the study.

87 Finally, to compare the capabilities of the two techniques, investigations after a dental treatment
88 are made, for both cavities and dental crowns.

89 2. Materials and Methods

90 2.1. Radiography

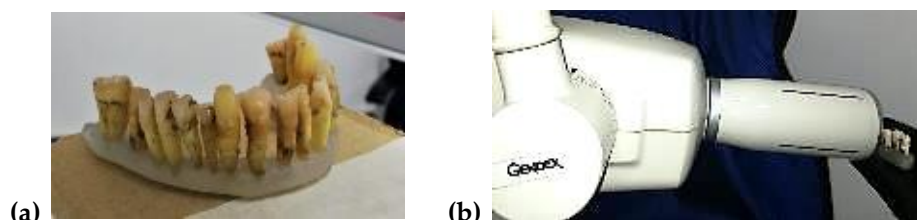
91 For this study, several extracted teeth were gathered from the *Dental Experts Clinic*, Timisoara,
92 Romania, following the Ethical protocol of the Clinic, with the written consent of the patients. All
93 teeth were extracted during different treatments, and not for the sole purpose of this study. While

94 such samples are *ex vivo* X-ray imaged (see Sections 3.2 and 3.3), other such investigations are
 95 performed *in vivo* in the above clinic, during clinical investigations, on bone and teeth in the oral
 96 cavity (see Section 3.1).

97 The radiological investigations with additional measurements are performed in the clinic using
 98 two radiological units: Planmeca ProMax 3D Plus (Planmeca, Helsinki, Finland) for panoramic
 99 radiography, and 3D CBCT, Gendex Oralix (Danaher Corporation, Washington DC, USA) for
 100 intraoral radiography [25] – Figure 1.

101 The maximum resolution achieved with both X-ray units has been 75 μm , after the optimizations
 102 described in detail in [9]. The protocol for obtaining such high-quality radiographs was optimized to
 103 comply with the *As Low As Reasonably Achievable* (ALARA) protocol [26]. This means that the X-ray
 104 unit provides the highest possible quality radiography, exposing the patient to the smallest possible
 105 amount of radiation. Intraoral radiography is performed at 68 kV and 9 mA for an exposure time
 106 between 0.5 and 1 s. Panoramic radiography and 3D CBCT have unchangeable exposure time of 15 s
 107 and 5 s, respectively. X-ray tube settings for panoramic radiography are 72-73 kV and 11 mA, while
 108 for 3D CBCT they are 90 kV and 14 mA, with an additional ultra-low dose (ULD) protocol.

109 To obtain high-quality images and to improve the radiographs, or to assess issues of treatments
 110 using them [27, 28], each X-ray unit is equipped with additional computing power. The Planmeca X-
 111 ray unit is part of a system with two additional PCs, all linked in a private network: the first one
 112 works as a server and for image reconstruction and the second one for image processing. The image
 113 reconstruction PC has an Intel Core i5 (6th generation) CPU, 16 GB RAM, an x64 based operating
 114 system, two memory disks (1 SSD with 128 GB storage space and 1 HDD with 1 TB storage space), a
 115 dedicated GPU with minimum 2GB RAM and a LAN connection. This PC collects the information
 116 from the sensor [9], processes and converts it into a raw 2D or 3D image. The image processing PC
 117 has an Intel Core i7 (6th generation), 16 GB RAM, an x64 based operating system, three memory disks
 118 (1 SSD with 256 GB storage space and 2 HDD with 1 TB storage space each, connected in a RAID1
 119 configuration), a dedicated GPU with minimum 2GB RAM and it should have 2 LAN connections.
 120 RAID1 means that the same information is written on both HDDs and it is protected if an HDD is
 121 damaged. Thus, all data are safe and remain stored on the other HDD.



122
 123 **Figure 1.** (a) Prepared teeth for X-ray investigations; (b) teeth positioned in the X-ray unit Gendex Oralix
 124 (Danaher Corporation, Washington DC, USA), ready for exposure.

125 2.2. Optical Coherence Tomography (OCT)

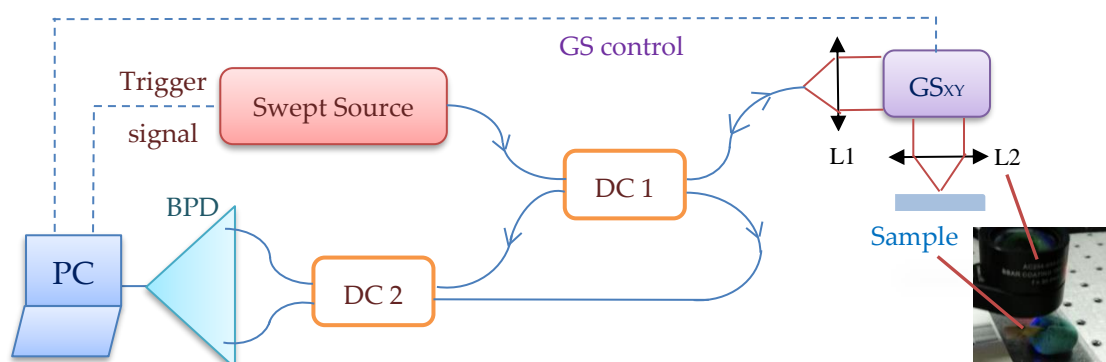
126 OCT investigations have been performed mainly using an in-house developed Swept Source
 127 (SS) OCT system, Master-Slave enhanced [7], (schematic diagram shown in Figure 2), at the “Aurel
 128 Vlaicu” University of Arad, Romania. It includes a 50 kHz laser source swept in frequency (Axsun
 129 Technologies Ltd, Billerica, MA, USA), with a centre wavelength of 1310 nm and a sweeping range
 130 from 1256.6 nm to 1362.8 nm. Its output optical beam (optical power 18 mW at the output of the laser)
 131 is directed towards an 80/20 directional coupler which conveys 20% of the source optical power
 132 towards the sample via a dual axis 2D galvanometer scanner (GS) [29]. The back-scattered light from
 133 the sample is guided back along the same path and is subsequently combined at coupler DC2 with the
 134 reference light. Each of the two DC2 arms leading to the balanced photodetector BPD (Santec Model
 135 BPD-200 DC) carries interference light resulting from the recombination of sample and reference light.
 136 They are converted into two electronic signals in opposite phase. The signal resulting from the
 137 difference operation is stripped of its DC slow varying component and its ac pulsates at an amplitude

138 twice of that of each photodetector signal due to the interference between sample and reference
 139 beams. This signal is further digitised by a 12-bit, 500 MS/s waveform digitizer model ATS9350
 140 (Alazartech, Quebec, Canada), converted to greyscale, put in a form suitable for viewing, and
 141 displayed using an in-house developed software, implemented in LabVIEW 2013, 64 bit. The same
 142 program also drives the 2D GSs via a data acquisition board model PCI 6110 (National Instruments,
 143 Austin, Texas). The acquired channelled spectra are used to build a 3D OCT image and produce C-
 144 scans/*en-face* images (situated at a certain depth in the sample), using the Master-Slave (MS) protocol
 145 [7]. This protocol allows for obtaining *en-face* images directly, without performing volumetric
 146 reconstructions first, using B-scans, as in conventional SS-OCT. The axial resolution provided by the
 147 instrument is 10 μm measured in air.

148 The OCT system use optical power at conservative level, as employed in imaging the retina, a
 149 few mW maximum, although larger power could be tolerated. At the level of safety values for the
 150 retina, sensitivity is 85-92 dB at 100 kHz line rates. For the Axsun source used in the setup in Figure
 151 2 (with 1310 nm and 50kHz), a sensitivity >97 dB is typically obtained with 3.6 mW optical power on
 152 the sample. There are numerous reports showing that MHz line rates are feasible within the power
 153 limitation due to safety, a few mW, hence similar speeds should be achievable in the applications
 154 concerned to this report, with immediate calculation in degrading the sensitivity proportional with
 155 the speed increase.

156 While in [7] the principle of MS has been first introduced using two interferometers, Master and
 157 Slave, the same study illustrated the implementation of MS using a single interferometer at two
 158 stages. As in practice, instead of a second interferometer (the Master one) a storage of channelled
 159 spectra can be employed, this is the main way MS is performed in this study, as well.

160 For some of the results presented in Section 3.4 on teeth and dental crowns, other two in-house
 161 developed OCT systems were used. These were a Spectral Domain (SD) and a Time Domain (TD)
 162 one, described in [30] and [31], respectively. Samples were extracted from patients attending the
 163 "Victor Babes" University of Medicine and Pharmacy of Timisoara, Romania, following an approved
 164 Ethical protocol and after their written consent.



165

166 **Figure 2.** In-house developed MS/SS-OCT system using a single interferometer at two stages.
 167 Components: Swept Source; DC_{1,2}, single mode directional couplers (20/80 and 50/50, respectively);
 168 GS_{xy}, dual axis galvanometer scanner; L_{1,2}, achromatic lenses; BPD, balanced photo-detector; PC,
 169 personal computer.

170 2.3. Characterization of samples

171 Several methods have been employed to characterize the samples of each group from different
 172 points of view, as briefly presented in the following protocol.

173 Extracted teeth are first analyzed with X-ray techniques since the radiology equipment is also
 174 located in the dental clinic that has provided (most of) the teeth for this study. After the teeth are
 175 extracted, they are cleaned and prepared for investigations. All types of radiographies are performed
 176 with all the available equipment in the clinic (common for such a medical environment): intraoral
 177 radiography, panoramic radiography, and 3D CBCT. In Figure 1 examples of teeth prepared for
 178 investigations are shown. Romexis Viewer (Planmeca, Helsinki, Finland) is the software utilized to

179 assess cavities or other dental issues. This is equipped with a toolbar that allows precise
180 measurements of dental aspects, even for images imported from other sources [32]. This is a novel
181 approach of this study, as most OCT studies are usually performed using an open source image
182 processing software, ImageJ (Wayne Rasband, NIH/LOCI, University of Wisconsin). In this study, to
183 make sure that differences in quantitative assessments are only related to the performance of the
184 techniques and not to software characteristics, the same software, Romexis Viewer is utilized.

185 After the image is provided by the X-ray unit or imported from another source (i.e., the SS-OCT
186 system), a calibration step is mandatory. This implies a correlation between the number of pixels and
187 the area of the surface, performed with the measurement toolbar, which also serves for calibration,
188 as well as for angles and lengths measurement [32]. However, we must note that, even if a software
189 is a trustworthy tool for accomplishing a correct assessment of an issue, it cannot surpass limitations
190 of the imported image's resolution. Thus, the software cannot be used to analyze details that cannot
191 be observed on radiographs.

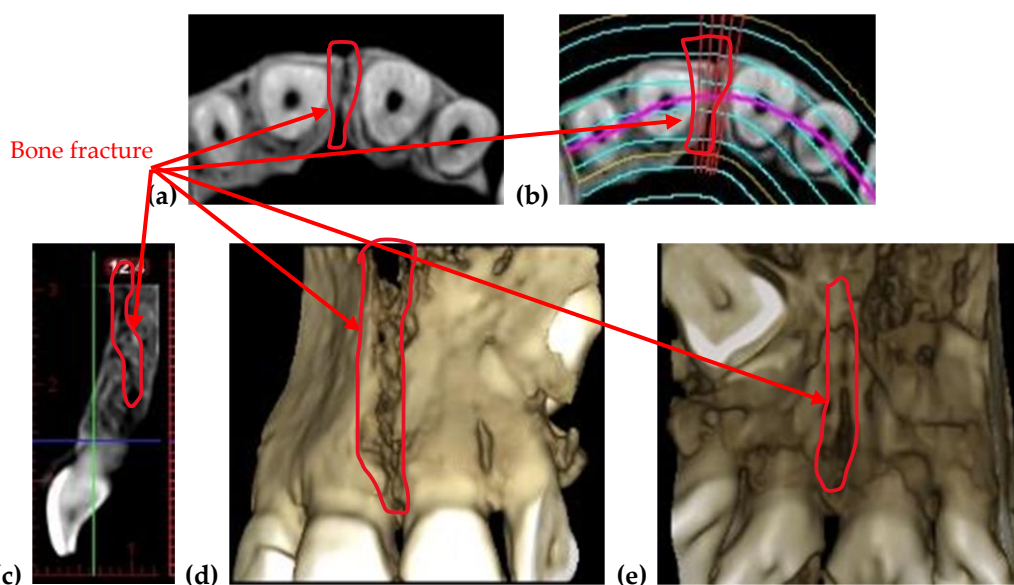
192 OCT investigations of different samples have been done using the MS/SS-OCT system in Figure
193 2, as well as (for a few samples) the SD and TD systems pointed out in the previous subsection. Teeth
194 need no preparation for OCT investigations, as they do not need any for X-ray radiography, as well.
195 500 OCT B-scans have been obtained for each sample from different lateral locations. They have been
196 further processed and analyzed with ImageJ, being rendered into a 3D image/volumetric
197 reconstruction. Where comparisons between radiography and OCT have been necessary, both B-
198 scans and 3D OCT images have been then imported in Romexis Viewer, for measurements and a
199 parallel study with radiographs.

200 3. Results and Discussion

201 3.1. Radiography-oriented dental investigations

202 Radiography is the daily-basis medical imaging technique in dentistry, therefore it is difficult to
203 select dental disorders that are visible only using this technique. From its variants, panoramic
204 radiography is the first method that can be (and is usually) performed, as it has the advantage of
205 providing an ample perspective of the full mouth of a patient in (only) a few seconds of investigation,
206

207 For a correct diagnosis, patients must be checked both clinically and radiologically. For bone
208 diseases (implying periodontitis or fractures) or for bone assessment, panoramic radiographs are not
209 necessary for density or post-operator investigations. A 3D CBCT has to be performed in such
210 situations because in addition to a qualitative assessment, it offers volumetric information. An
211 example of a CBCT investigation performed in the clinic for a fractured maxillary is presented in
Figure 3.

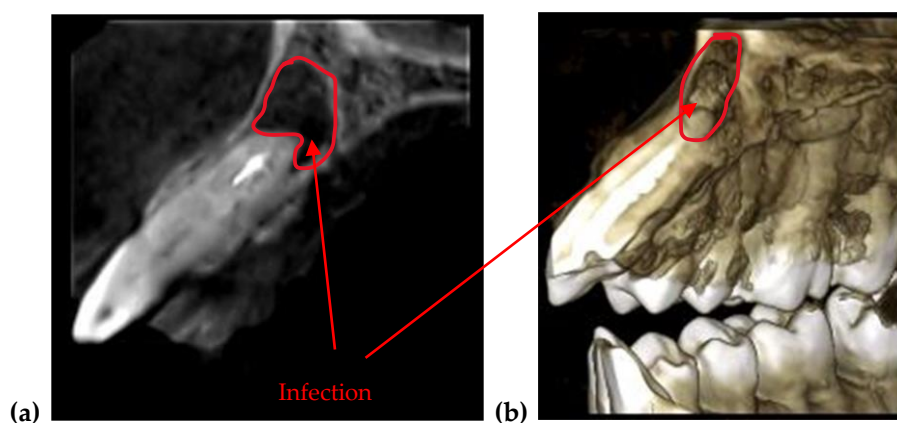


213 **Figure 3.** 3D CBCT of a fractured maxillary in different views: (a) axial view; (b) axial view indicating
214 the position of the fracture; (c) sagittal view; 3D reconstruction, (d) frontal and (e) posterior view,
215 previously detailed in [28]. Patient V.L., female, age 29 years, diagnosed with a crack in her maxillary
216 bone caused by a head trauma.

217 One can remark that in such cases OCT cannot be of use, as the necessary depth of the
218 investigation is beyond its capability. However, the crack in Figure 3 is also large enough for the
219 CBCT resolution to be sufficient to spot and assess its dimensions.

220 3D CBCT is also recommended when it is important to assess the tip of the tooth's root, as
221 presented in Figure 4. In such cases intraoral and panoramic radiographs do not offer reliable
222 information because they provide 2D images and if a dental infection is behind the tooth, it is not
223 visible. Such investigations are beyond the penetration capability of OCT, as well.

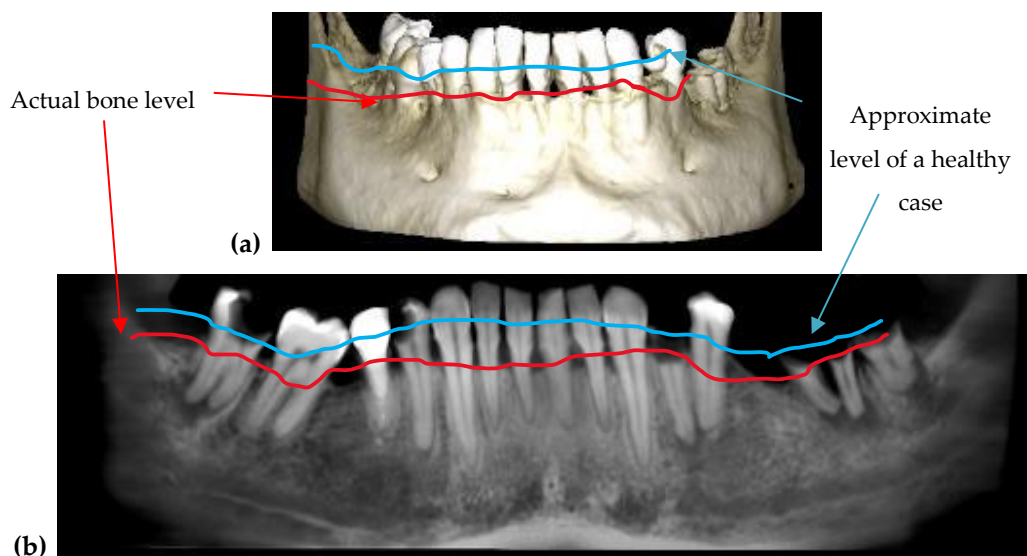
224 The periodontitis disease, in its advanced stages, can be diagnosed using any type of
225 radiography. Figure 5 is an example of periodontitis disease observed on both 2D and 3D
226 radiography. The red line represents the actual level of bone that is affected by the disease and the
227 blue line represents approximately the level where the healthy bone should be. The issue is to detect
228 it in (very) early stages, if possible, to apply appropriate treatments before the gingiva has begun to
229 retreat.



230

231 **Figure 4.** (a) Sagittal view and (b) 3D CBCT reconstruction of an infection formed at the tip of a tooth.

232 Patient C.B.G., female, age 37 years, diagnosed with dental abscess.



233

234

235

236

Figure 5. Periodontitis disease observed on a 3D CBCT reconstruction (a) and on a panoramic radiography (b). Patient C.O., male, age 34 years, diagnosed with periodontitis, alongside other dental issues such as cavities and dental abscesses.

237

238

239

240

241

242

243

While a range of methods can be used for diagnose, from periodontal probes [33] to 3D CBCT with high resolution and low radiation dose [34, 35], different biomaterials such as nanoparticles are considered to improve the performance in detecting and measuring periodontal pockets [36]. In this respect, making successive OCT investigations of the same area every 6 months can be relevant for the clinician regarding the success of the treatment. This can be in a similar way to using (*ex vivo*) holography on models to make such assessments [37]. A comparison of these two techniques in this respect is subject of future work.

244

245

246

247

248

249

250

251

252

253

254

255

256

257

258

259

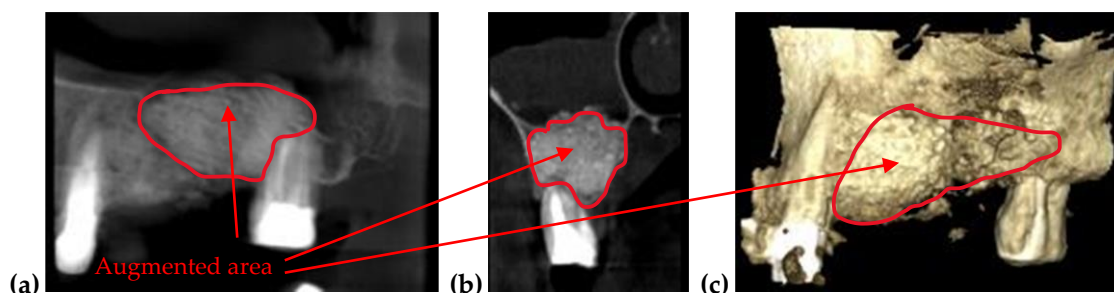
260

261

262

263

Augmented bone is necessary to provide enough jawbone volume for a successful dental implementation [38,39]. As various diseases (including trauma, cancers or osteoporosis) occur, the alveolar ridge must be augmented (Figure 6), because there is not enough bone left to use implants. Allografts or autografts may be utilized, although the former may transmit certain diseases, while the latter involves additional clinical procedures and increases morbidity. Alternate materials such as bioceramics are developed for such scaffolds [40], while procedures such as photo-biomodulation/Low-Level Laser Therapy (LLLT) are demonstrated to accelerate new bone formation when additional bone particles are utilized to stimulate bone regeneration. For the latter we have used OCT to demonstrate the positive impact of LLLT on new bone formation [41]. The advantage of OCT is its capability to monitor *in vivo*, non-invasively the process (in contrast to micro-CT or the gold standard of histopathology [42]), and with higher resolution than radiography. The OCT's drawback in this case as well is its lower penetration depth and Field-of-View (FOV), (the latter imposing mosaicking images [43] or segmenting investigations [41]), while radiography has both enough penetration depth and FOV to assess the results of the bone-augmentation process, as shown in the example considered in Figure 6. Because of this disease, the patient lost several teeth that cannot be replaced with dental implants because of the patient's insufficiency in bone quantity and density. To make possible the surgery of implants insertion, the patient was subjected to an additional surgery of bone augmentation. The augmentation was made with Geistlich Bio-Oss (Wolhusen, Switzerland), which is a natural bone mineral of bovine origin that is available as granules of spongy bones in an applicator.



264

265

266

267

Figure 6. (a) Panoramic view, (b) sagittal view, and (c) 3D reconstruction of an augmented bone obtained after a segmental 3D CBCT with a FOV of 5 x 5 cm. Patient P.P., male, age 46 years, diagnosed with severe periodontitis.

268

3.2. OCT-oriented dental investigations, compared with radiographs

269

270

271

272

273

274

Cavities assessment, enamel or dentine issues such as cracks or demineralization, adaptation of dental fillings or crowns are examples of several dental affections that can be better assessed on OCT images than on any type of radiography, as documented by different groups [10-15, 44-46], including ours [17, 28, 47]. The investigations in Figures 7 to 14 on examples of such dental issues prove that OCT images allow for a more accurate diagnosis than radiographs in several situations, where resolution is paramount, and the penetration depth of OCT is enough.

275

276

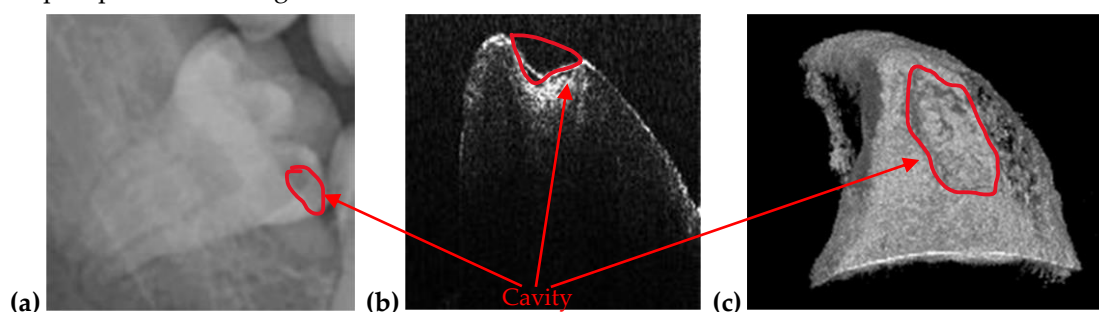
277

278

279

280

Figure 7 is an example of the superior resolution and contrast of OCT images. This can be best seen on a volumetric/3D reconstruction in Figure 7(c), but also on a well-chosen cross-section/B-scan in Figure 7(b). In contrast, in the radiograph in Figure 7(a), the (large) dental cavity can barely be spotted. As demonstrated in the following section, such cavities can be exactly measured on OCT images, while on radiographs they can only be observed. Similar remarks can be made regarding the examples presented in Figures 8 and 9.



281

282

283

284

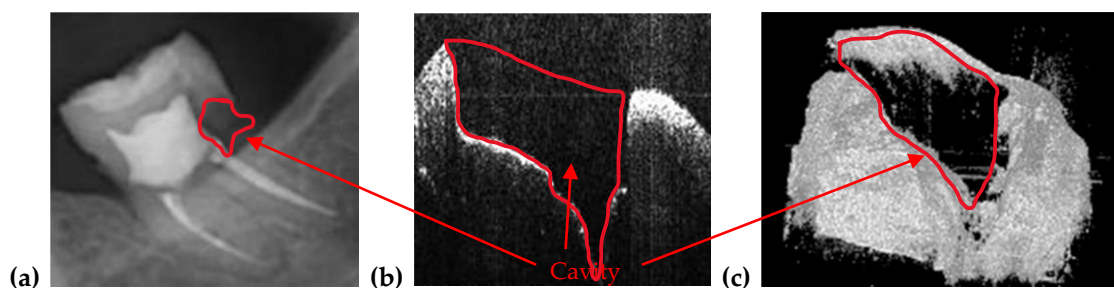
285

286

287

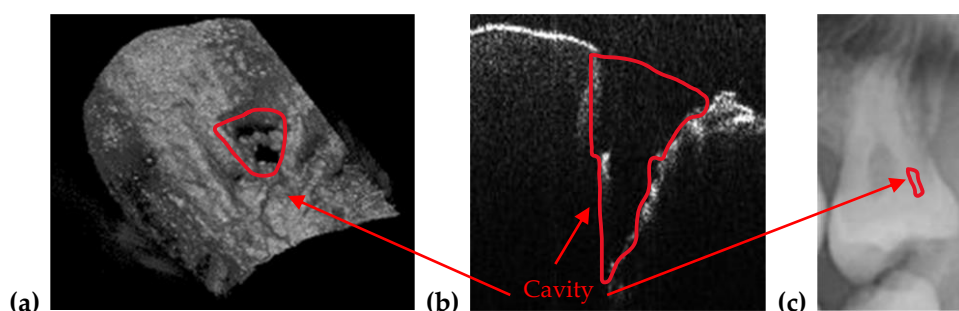
288

Figure 7. (a) Cavity of a third molar from the fourth quadrant assessed on a section cropped from a panoramic radiography. OCT investigation on the tooth extracted for medical purposes after performing the radiography: (b) B-scan and (c) 3D reconstruction. Patient E.M., male, age 23 years, diagnosed with a cavity on the smooth surface (lateral side) of the third molar, with the following remarks on the clinic condition: the cavity appeared because the third molar is not in a correct position and in that area, between the second and the third molar, the patient cannot perform a full cleaning of the tooth.



289

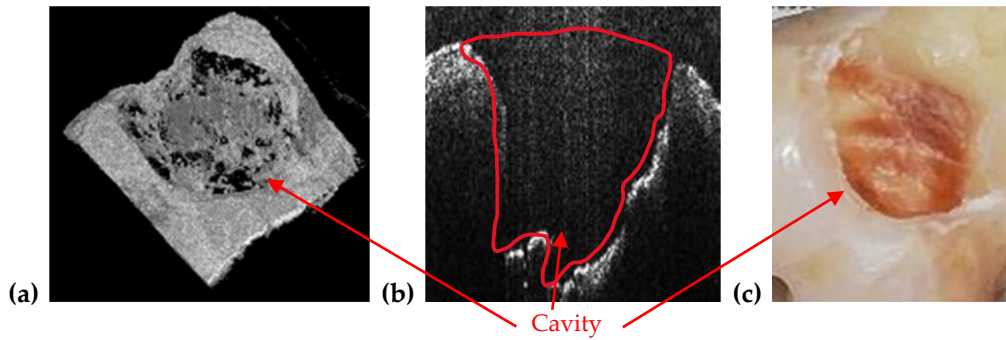
290 **Figure 8.** Cavity of a second molar from the third quadrant assessed on (a) a section cropped from a
 291 panoramic radiography. OCT investigation on the tooth extracted for medical purposes after
 292 performing the radiography: (b) B-scan and (c) 3D reconstruction. Patient M.N., female, age 29 years,
 293 diagnosed with a cavity on the smooth surface of the tooth and one of the tooth's root. The latter is so
 294 large because there are two cavities connected with each other: The first one is a recurrent cavity that
 295 appeared under the filling because of an endodontic treatment; the second one appeared because of the
 296 receding gingiva and mandibular bone, which has left the tooth exposed.



297

298 **Figure 9.** Cavity of a third molar from the second quadrant assessed on: (a) an OCT 3D reconstruction
 299 and (b) an OCT B-scan, both performed on the tooth extracted for medical purposes after performing
 300 the radiography; (c) a section cropped from a panoramic radiograph. Patient C.M., male, age 24 years,
 301 diagnosed with a small cavity, with the following remarks on his clinic condition: the tooth did not pass
 302 completely from the gingiva, but food, as well as degenerative factors entered between tooth and
 303 gingiva. This is the reason the cavity has appeared.

304 In the example in Figure 10, the precision of OCT technique when it comes to imaging dental
 305 cavities can be remarked by analyzing Figure 10(a) and (b). The margins of OCT 3D rendering in
 306 Figure 10(a) is 1:1 with the margins obtained from the photography in Figure 10(c). This is one of the
 307 reasons that makes OCT the appropriate medical imaging technique when it comes to investigate
 308 cavities. Alongside its superior accuracy, OCT is radiation-free. Regarding the acquisition speeds,
 309 they are from 1 to 15 s for different types of radiographs (as pointed out in Section 2.1), while for OCT
 310 they are much faster, usually in milliseconds-for a common individual scan, with the FOV
 311 corresponding to an area of up to $3 \times 3 \text{ mm}^2$. If mosaic OCT images are performed [43], the acquisition
 312 time can be longer, but less than 1 s in all situations. For the MS enhanced SS-OCT system used in
 313 this study (Figure 2), OCT imaging is also performed in real time, with no post-processing of images.

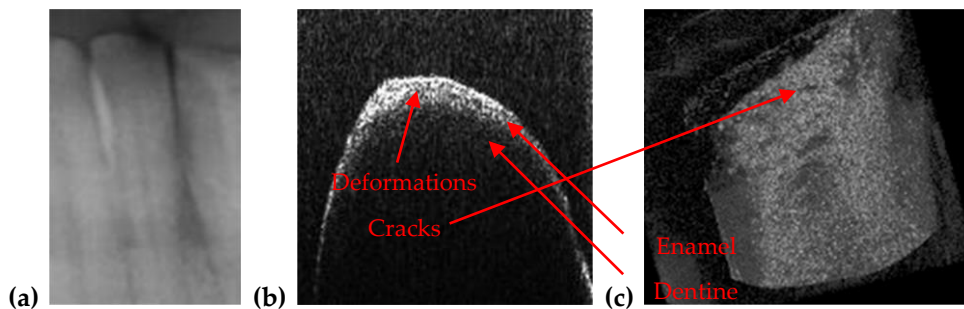


314
315
316
317
318
319

Figure 10. Cavity of a third molar from the second quadrant assessed on (a) an OCT 3D reconstruction and on (b) an OCT B-scan. Image (c) is a photograph of the cavity. Patient R.E., male, age 27 years, diagnosed with a large cavity formed at the border between a dental crown and the tooth’s root. The reason for this cavity is the impossibility of the patient to clean that area because of the gingiva and the inner cheek thickness.

320
321
322
323
324
325

Beside cavities, OCT is capable to detect abnormalities at the level of enamel and dentine. As demonstrated in the examples in Figures 11 to 14, because of its high resolution, OCT images reveal dental issues such as enamel deformations or cracks. Figure 11(b, c) reveal enamel deformations at the cusp of the tooth and some small cracks on the smooth surface of the tooth. Figure 11(a) is a section of a panoramic radiography, and the issues visible on OCT images are not spotted at all on the panoramic radiography.

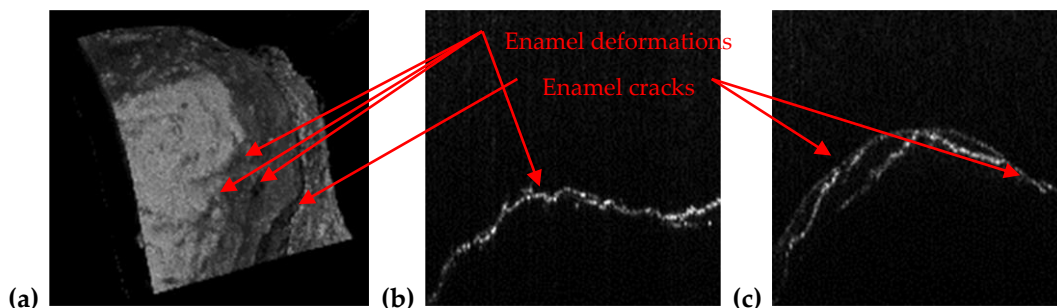


326
327
328
329
330

Figure 11. Enamel deformations of an incisive tooth from mandible that cannot be observed on a section cropped from a panoramic radiography (a) but can be clearly remarked both on (b) OCT B-scans and on (c) a 3D OCT reconstruction (performed on the tooth extracted for medical purposes after performing the radiography).

331
332
333
334
335
336
337

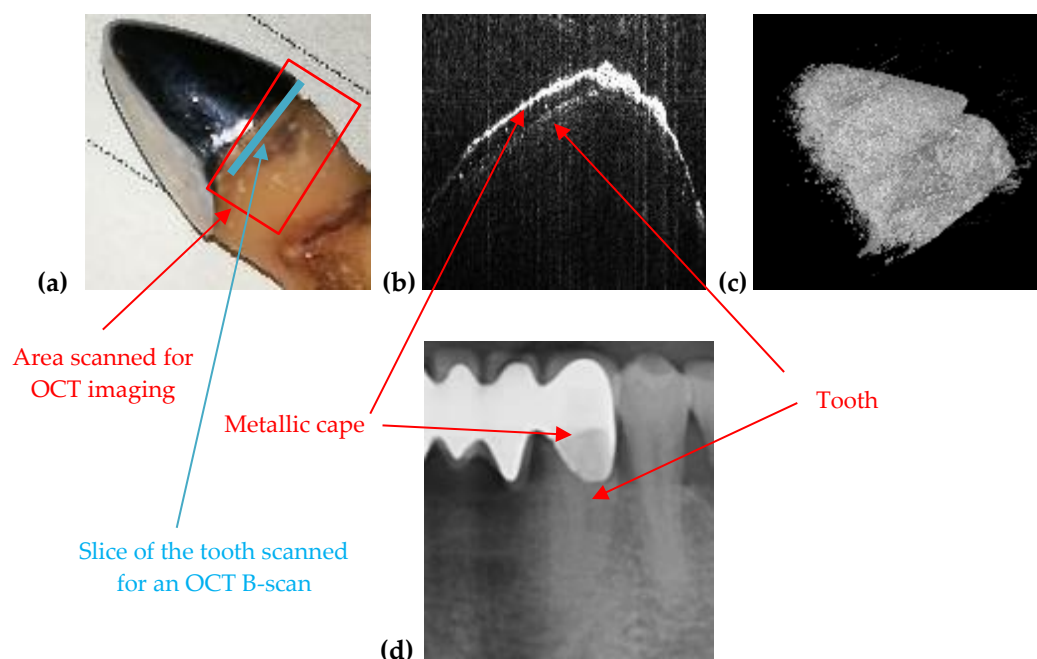
Figure 12 is also revealing enamel deformations and cracks on a smooth surface of an incisive tooth. In this case, these dental aspects are more visible using OCT than in the case in Figure 11; in the panoramic radiography they are not even spotted. As a remark, compared to such classical structure-oriented OCT, polarization sensitive (PS) OCT can provide much higher contrast on enamel deformations or demineralization in the enamel [48]. Therefore, applying PS OCT for such dental issues can be a valuable direction of future work. Images of the teeth from Figures 11 and 12 belong to the same patient, T.C., male, age 34 years, diagnosed with advanced periodontitis.



338

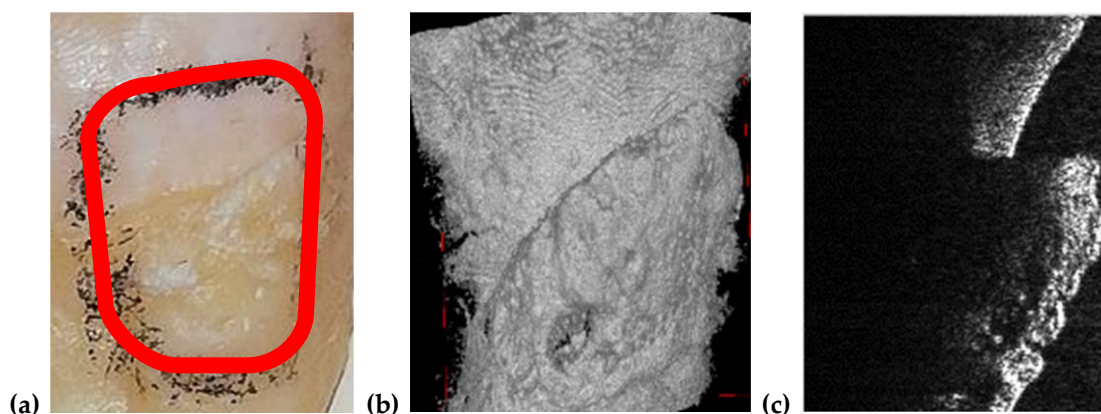
339 **Figure 12.** Enamel deformations and cracks of an incisive tooth observed on (a) OCT 3D reconstruction,
 340 as well as on (b, c) different B-scans.

341 Another situation where OCT is better suited than X-ray imaging is when the adaptation of dental
 342 crown on the abutment prepared tooth must be checked. Figure 13 is showing an example of a tooth
 343 with a metallic cape. The adaptation of this cape is visible only on OCT images, Figure 13(b). Figure
 344 13(d) is a section cropped from a panoramic radiograph, and one can see that on this image the
 345 adaptation cannot be assessed. In Figure 13(b) one can observe the metallic layer and the tooth
 346 because the OCT B-scan is obtained at the junction between these two components, marked with the
 347 blue line in Figure 13(a). In the area where the metallic cape is scanned, one cannot see the tooth
 348 because the IR laser radiation specific to OCT does not pass through metallic surfaces. Figure 13(c) is
 349 the OCT 3D reconstruction of this selected area marked in Figure 13(a).



350 **Figure 13.** OCT used to check the adaptation of metallic cape on the tooth: (a) photo of the tooth with
 351 cape, (b) OCT B-scan showing both the tooth and the metallic cape, (c) 3D reconstruction, and (d)
 352 section cropped from a panoramic radiography. Patient S.S., female, age 57 years, diagnosed with
 353 multiple abscessed teeth and periodontitis.
 354

355 In Figure 14 a deep crack in a tooth is imaged. While the crack can be observed visually, Figure
 356 14(a), its depth can be assessed quantitatively using OCT images, choosing the appropriate B-scan,
 357 Figure 14(c), from the 3D OCT reconstruction of the zone of interest, Figure 14(b).



358 **Figure 14.** Deep crack in the enamel layer observed on (a) part of the photo of an extracted tooth, as
 359 well as on (b) the 3D OCT reconstruction of the selected area. (c) OCT B-scan showing the shape of the
 360

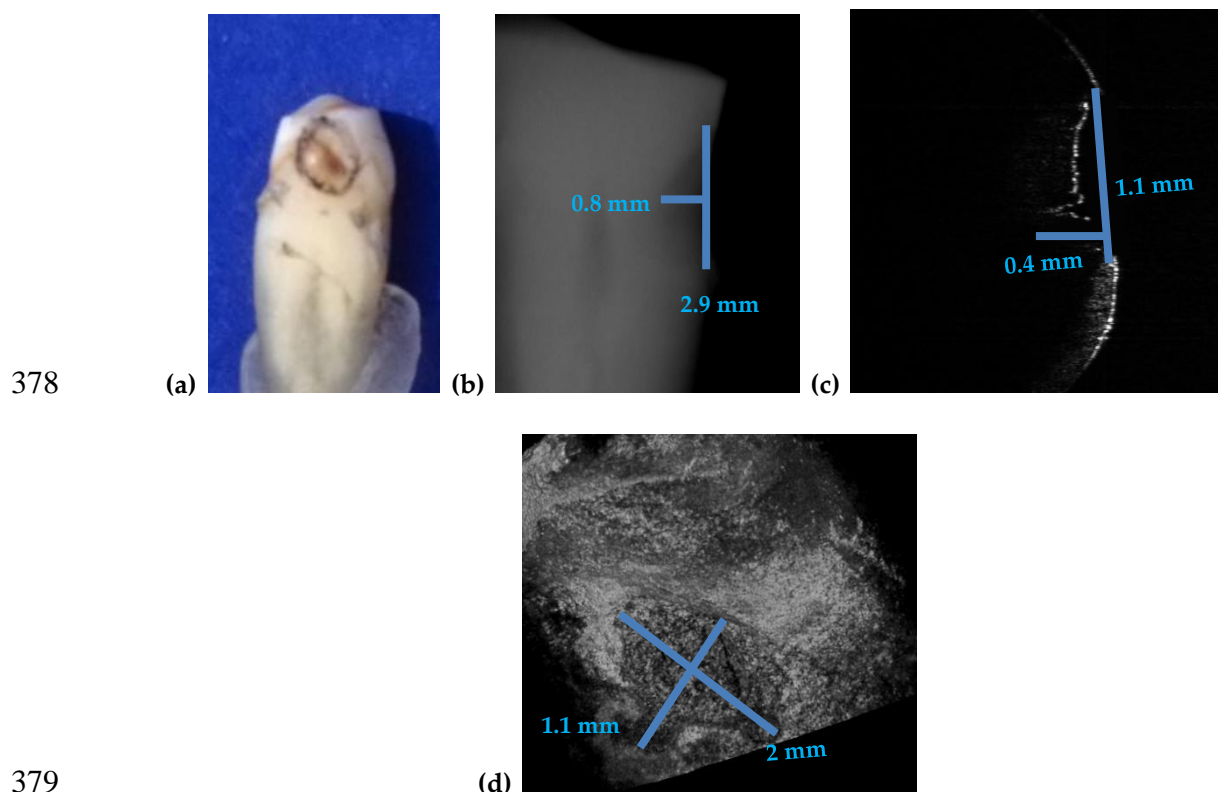
361 crack. If necessary, the dimensions (especially the depth) of the crack can be accurately measured on
 362 such a B-scan. Patient C.T., male, age 23 years, diagnosed with several dental problems on a third molar
 363 (i.e., gingiva inflammation, abscess, cavities, and wrong growth of the tooth).

364 3.3. Measuring dental cavities on both OCT images and radiographs

365 The aim of this section is to utilize OCT images to see if one can diagnose clear margins of
 366 cavities. These results are compared with those obtained with radiographs. One must point out in
 367 this respect that, even if the resolution is the same for any type of radiography, there are differences
 368 in the details that can be observed on the acquired images. For example, a small cavity cannot be
 369 diagnosed exactly on a panoramic radiography, but an intraoral radiography delivers more detailed
 370 information. The advantage of the intraoral radiography over panoramic radiography in the case of
 371 a small cavity is related to the fact that for the former the focus is on that part of the mouth where the
 372 tooth with a specific affection is located [27].

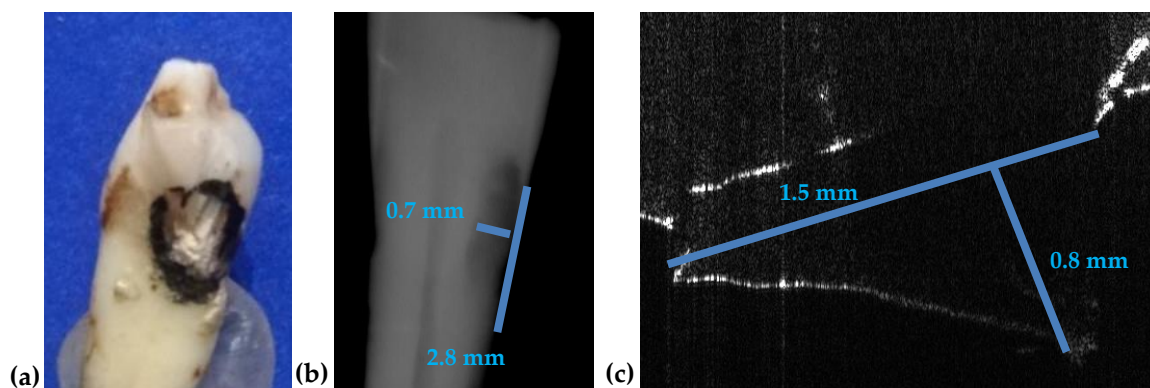
373 A few relevant examples of cavities are considered to make such a comparison in Figures 15 to
 374 17, which show that measurements on intraoral radiographs give results different than those on OCT
 375 images.

376 For the case presented in Figure 15, there is a difference of 0.9 mm in length and the depth is
 377 double on the intraoral radiograph as compared to the OCT image.



380 **Figure 15.** (a) A premolar tooth, with an area marked for OCT investigations; (b) section cropped from
 381 an intraoral radiograph with a view on the measured dental cavity; (c) OCT B-scan, where the depth
 382 and the width of the cavity are measured; (d) volumetric OCT reconstruction, on which the width and
 383 the length are measured.

384 For the case presented in Figure 16, the difference between the measurements of the length on
 385 both images is 1.3 mm while the difference for depth measurements is 0.1 mm. Measurements errors
 386 from Figure 15(b) and 16(b) are therefore significant. We point out that the values obtained using
 387 OCT images are the correct ones because they have been checked by direct measurements.



388

389

390

391

Figure 16. (a) Incisive tooth with an area marked for OCT investigations; (b) a section cropped from the intraoral radiography with measurements of the cavity; (c) OCT B-scan where the depth and the length measurements of the cavity have been performed.

392

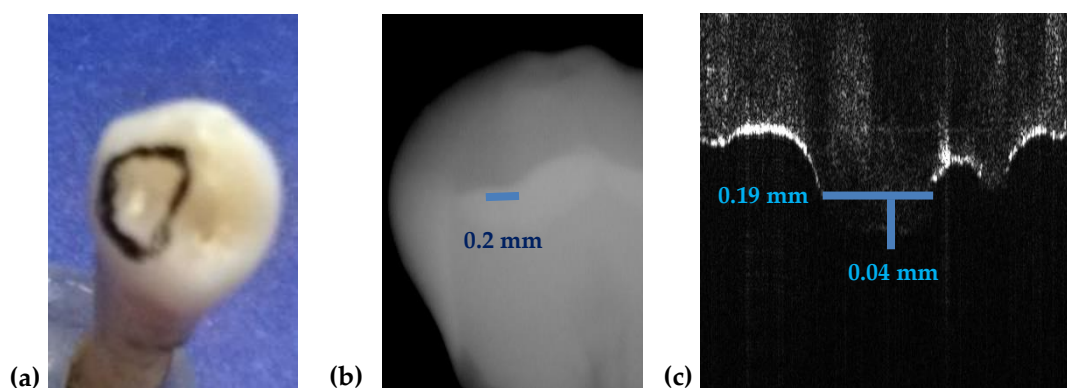
393

394

395

396

The case presented in Figure 17 consists of a small cavity that is barely visible on intraoral radiography. The fact that an estimation using the radiograph gives only 0.01 mm in difference from the value obtained using the OCT image is merely a coincidence. There is no way to correctly measure the cavity on an intraoral radiograph (in depth, length, or width) while Figure 17(c) proves that on the OCT B-scan one can properly perform measurements.



397

398

399

400

Figure 17. (a) Canine tooth, with an area marked for OCT investigations; (b) a section cropped from the intraoral radiography where the cavity was measured; (c) OCT B-scans with measurements of depth and width of the cavity.

401

402

403

404

405

406

407

408

409

410

411

We may conclude that cavities can be identified and measured with both techniques but can be correctly assessed in terms of their dimensions using OCT only. Furthermore, there are new (early) cavities that cannot be observed on radiographs, but that can be spotted on OCT images—as concluded in our preliminary work in [17]. Intraoral radiographs and OCT images can be both utilized for diagnosis of dental cavities but the most accurate method for quantitatively assessing dental cavities proves to be OCT. Histopathology, which is the “gold standard” in microscopic examinations, could have been an option to compare with both radiography and OCT. However, in this case we address only dimensional measurements on (the surface of) teeth, and not cell-level evaluations of tissue.

Following these ascertainties, a comparison has been made between the measuring accuracy of the different dimensions of the detected cavities, using the two methods. The results are presented, for the examples considered in the paper, in Table 1.

412 One can observe that there is no column *width* for the *radiography* assessment, because for
 413 measuring cavities intraoral and panoramic radiographs are utilized, and they are 2D images. The
 414 relative error

$$415 \quad \varepsilon (\%) = \frac{|x_{\text{Radiography}} - x_{\text{OCT}}|}{x_{\text{OCT}}} \cdot 100 \quad (1)$$

416 is calculated in all the cases where data has been available with both imaging techniques, where
 417 $x_{\text{Radiography}}$ is the length or depth measured on radiographs and x_{OCT} is the length or depth
 418 measured on OCT images.

419 **Table 1.** Measurements performed on both radiography and OCT images obtained for the same tooth.

Measurements on tooth from	Radiography		OCT			Relative error ε (%)	
	Length (mm)	Depth (mm)	Length (mm)	Width (mm)	Depth (mm)	For length	For depth
Figure 7	3.2	1.6	1.9	0.8	0.5	68	110
Figure 8	2.4	2.2	3.0	2.7	3.3	20	33
Figure 9	1.5	1.9	2.0	0.9	3.3	75	42
Figure 10	2.7	3.0	3.5	3.9	3.8	34	21
Figure 15	2.9	0.8	2	1.1	0.4	45	100
Figure 16	2.8	0.7	1.5	-	0.8	86	12
Figure 17	0.2	-	0.19	-	0.04	5	-
Mean relative error $\bar{\varepsilon}$ (%)	$\bar{\varepsilon} = \frac{\sum_{j=1}^N \varepsilon_j}{N} = 50\%, \quad (2)$ where N=13 is the number of relative errors for measurements performed with both methods.						
Standard Deviation of relative errors σ (%)	$\sigma = \sqrt{\frac{\sum_{j=1}^N (\varepsilon_j - \bar{\varepsilon})^2}{N-1}} = 34.3\% \quad (3)$						

420 For these errors, the mean value and the Standard Deviation are calculated in Table 1. One can
 421 see the quite large value of the mean, due to the large errors made in radiographic measurements (on
 422 images that do lack resolution, but also contrast). There is also a large standard deviation for these
 423 relative errors, because some measurements can be made more precisely on radiographs, while others
 424 are significantly flawed. We may conclude that only OCT images present enough resolution to allow
 425 for such accurate assessments.
 426

427 Two imaging characteristics that must be discussed are contrast and sharpness. To compare
 428 images obtained with two different methods, the measurements are performed using a single
 429 software. The differences between the images of each sample can be quantified by analyzing the data
 430 provided by the Romexis software. Table 2 presents the values gathered for each of the above 2D
 431 image. One must remark that 3D CBCT images are adjustable in terms of contrast and brightness
 432 from 0 to 4095, and sharpness from 0 to 10.

433 *The contrast* is calculated with the equation [1]

$$434 \quad C = (I_{\text{max}} - I_{\text{min}}) / (I_{\text{max}} + I_{\text{min}}), \quad (4)$$

435 where I_{max} and I_{min} are the maximum and minimum pixel intensity, respectively.

436 *The Contrast-to-Noise Ratio (CNR)* can be also calculated using the equation [1]

$$437 \quad \text{CNR} = \frac{|I_{\text{min}} - I_{\text{max}}|}{\sigma_0} \quad (5)$$

438 where σ_0 is the standard deviation of the pixel intensity I , and it is provided by the imaging software.
 439 Their values are provided in Table 2 for each of the two methods, comparatively, when both are
 440 available for a certain sample investigated in this study (and only for one of the methods, when only
 441 one of them is available). This comparison allows for calculating the relative error for each sample
 442 and parameter, like the calculus performed in Table 1 for the measured dimensions of the cavities. A

443 mean relative error and its standard deviation can be then obtained for each of the two parameters
 444 (Table 3).

445 **Table 2.** Measurements of Contrast (C) and Contrast-to-Noise Ratio (CNR) performed on radiography
 446 and OCT images obtained for each sample considered in the study.

Sample from Figure	Imaging method	Maximum and minimum pixel intensity I		σ_0 (%)	C	ϵ_C^j (%)	CNR	ϵ_{CNR}^j (%)
		I_{max}	I_{min}					
7	OCT	255	1	71.7	0.992	98.4	3.54	4.1
	Panoramic	192	64	37.57	0.5		3.4	
8	OCT	255	1	92.25	0.992	41.7	2.73	13.8
	Panoramic	208	31	55.7	0.74		3.17	
9	OCT	255	1	53.82	0.992	86.8	4.71	54.9
	Panoramic	193	59	44	0.531		3.04	
10	OCT	255	2	55.15	0.984	-	4.58	-
11	OCT	255	5	45.42	0.961	45.1	5.5	27.6
	Panoramic	123	25	22.7	0.662		4.31	
12	OCT	255	0	45.25	1	51	5.63	30.6
	Panoramic	123	25	22.7	0.662		4.31	
13	OCT	255	9	94.76	0.931	37.7	2.59	33.7
	Panoramic	238	46	49	0.676		3.91	
14	OCT	255	4	89.8	0.969	-	2.79	-
15	OCT	188	0	26.7	1	16.8	7.04	55.1
	Panoramic	232	18	47.11	0.856		4.54	
16	OCT	255	0	44	1	16.8	5.79	27.5
	Panoramic	232	18	47.11	0.856		4.54	
17	OCT	255	2	70.3	0.984	14.9	3.59	20.9
	Panoramic	232	18	47.11	0.856		4.54	
Mean relative error of C ($\bar{\epsilon}_C$)		$\bar{\epsilon}_C = \frac{(\sum_1^N \epsilon_C^j)}{N} = 45.46\%, \quad (6)$ where N=9 is the number of relative errors for measurements performed with both methods.						
Standard Deviation of the relative errors of C (σ_C)		$\sigma_C = \sqrt{\frac{\sum_1^N (\epsilon_C^j - \bar{\epsilon}_C)^2}{N-1}} = 29.9\% \quad (7)$						
Mean relative error of CNR ($\bar{\epsilon}_{CNR}$)		$\bar{\epsilon}_{CNR} = \frac{(\sum_1^N \epsilon_{CNR}^j)}{N} = 29.8\%, \quad (8)$ where N=9 is the number of relative errors for measurements performed with both methods.						
Standard Deviation of the relative errors of CNR (σ_{CNR})		$\sigma_{CNR} = \sqrt{\frac{\sum_1^N (\epsilon_{CNR}^j - \bar{\epsilon}_{CNR})^2}{N-1}} = 16.93\% \quad (9)$						

447 From Table 2, the difference in contrast between OCT images and radiographs is significant,
 448 with a mean relative error of 45.46%. This means that OCT images have better contrast. This was
 449 expected because OCT images are performed directly on the tooth, while for radiographs there are
 450 other anatomical elements (i.e., bone, gingiva, tongue, cheek, jaw, lips, etc.) that appear on the image
 451 and influence the contrast. The mean difference between the contrast values of OCT images and
 452 radiographs from cases where radiographs were performed on patients (Figure 7, 8, and 9) is 0.40,
 453 while the mean difference in the cases where radiographs were performed on extracted teeth (Figure
 454 15, 16, and 17) is 0.13. This proves that soft and hard tissues existing around the tooth influence the
 455 contrast.

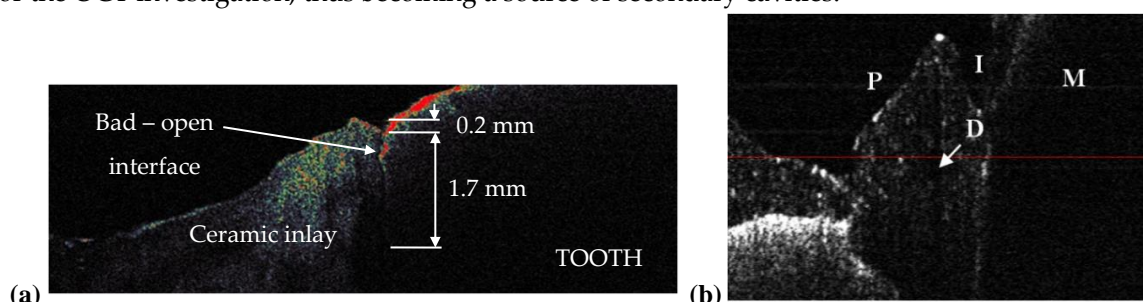
456 The mean relative error of CNR is 29.8%, and it is smaller than the value of the mean relative
 457 error of contrast. This means that images have good sharpness, even if in several OCT images (Figure
 458 10, 13, and 17) and radiographs (Figure 13, 15, and 16), different artefacts are visible. Any metallic

459 surface or a material that has great reflexivity is producing artefacts when OCT investigations are
 460 performed around that area. Also, metallic surfaces influence contrast and sharpness of radiographs
 461 because they absorb X-ray radiation; thus, sometimes image reconstruction artefacts appear. Figure
 462 13 is an example of such a situation where the metallic cape produces artefacts on both OCT images
 463 and radiographs.

464 3.4. Treatment assessments using OCT

465 Three examples on the capability of OCT to perform dental treatment assessments are provided
 466 in Figures 18 to 20. Numerous other such examples have been reported in our previous studies [47].
 467 Such applications have also been considered from the late 1990s, including in early studies of OCT in
 468 dentistry [10, 11].

469 The most common dental treatments that can be targeted using OCT are related to cavities. As
 470 shown in Figure 18(a), an OCT B-scan (i.e., a cross-section inside the teeth) can reveal defects both in
 471 the inlay introduced in the dental cavity and in the interface between the tooth and the added inlay.
 472 The capability of OCT in this respect is unique: an interface defect may not appear on the tooth surface
 473 or it may look superficial, as in Figure 18(a). However, using the non-invasive IR laser-based OCT
 474 investigation, one remarks on the OCT B-scan that the (open) interface has not just a 0.2 mm surface
 475 defect, but a (precisely evaluated) 1.7 mm depth defect. The latter would go unnoticed if it were not
 476 for the OCT investigation, thus becoming a source of secondary cavities.



477 (a) OCT B-scan of a treated dental cavity obtained with an in-house developed 1D GS-based
 478 OCT handheld probe [30, 48], which allows for the evaluation of the interface between a tooth and the
 479 ceramic inlay: apparently good interface, closed, but with a crack between tooth and inlay; (b) OCT B-
 480 scan of a metal ceramic dental prosthesis using the same 1D GS-based handheld probe and an SD-OCT
 481 system [48], with the following notations: M, 1st molar (M); P, 1st premolar; D, defect in the ceramic
 482 layer; I, interface between M and P.
 483
 484

485 The question is: can such an assessment be made using the common (and most utilized)
 486 radiography? The answer is negative, as we have demonstrated in detail in [31]. On the other hand,
 487 OCT can perform this task, as both the necessary resolution and penetration depths are fully within
 488 its capabilities. An example in this respect is shown in Figure 19, in an investigation similar to those
 489 in [31]: *ex vivo*, on half of a tooth, sectioned and observed with optical microscopy in Figure 19(a).
 490 Early cavities cannot be measured (and some cannot even be remarked) on radiographies, nor can be
 491 assessed issues of the dental treatment. In contrast, OCT allows for such an evaluation, as shown in
 492 Figure 19 on the entire 3D OCT reconstruction (b), on its occlusal view (c) or using B-scans, as in the
 493 (d, e, f) sections. Another view of interest available with OCT is in the *en-face* image/C-scan, such as
 494 the one in Figure 19(g), obtained from the 3D OCT image by sectioning it with a plane situated at a
 495 certain (constant) depth—in this case from the occlusal surface of the tooth. Using the MS enhanced
 496 OCT technique [7], such *en-face* OCT images can be obtained directly, without having to retrieve
 497 3D/volumetric reconstructions first. They can be used to obtain a more complete view on the location
 498 and extension of defects, as detailed in [31], as well.
 499

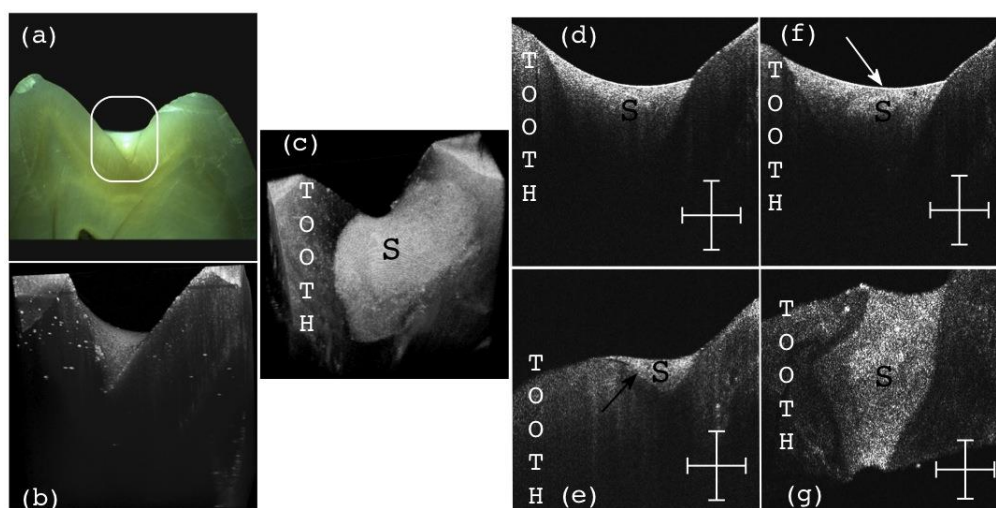


Figure 19. OCT B-scan of a treated dental cavity: **(a)** area of interest; **(b)** 3D OCT reconstruction after the investigation showing the mentioned area; **(c)** general aspect of the sealant (S) from the occlusal view; **(d)** B-scan of the structure presenting a good interface between the tooth enamel and the sealant (S); **(e)** B-scan presenting an open interface (black arrow) between the sealant (S) and the tooth structure; **(f)** B-scan presenting a defect (white arrow) inside of the sealant material; **(g)** C-scan of the structure presenting no defects inside the sealant (S) material at the considered depth; Scale bars: 1 mm.

Other aspects can be revealed as well, using OCT, for example regarding the nature of the material of the sealant (S) utilized for the cavity treatment. A ceramic inlay can thus be clearly seen differently from a polymeric one because of their different porosity [49].

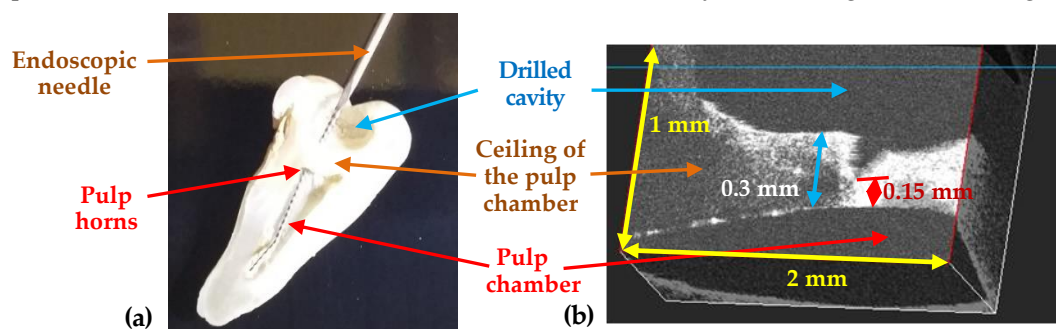
Furthermore, OCT investigations can be also performed *in vivo*, using handheld scanning probes. Such probes have been developed using 2D GSs [50, 51], 2D Micro-Electro-Mechanical Systems (MEMS) [51, 52], or, for Dental Medicine, even a simple 1D GS (lower-cost and light-weight). Such a 1D GS-based handheld probe [30, 49]) can be utilized for such applications even if it provides only a single B-scan at the time, because the dentist is providing the second direction of lateral scanning by moving the probe across the area of interest (for example the tooth surfaces), thus monitoring in real time on a PC screen successive B-scans. The dentist can thus assess a performed treatment by sweeping the tissue and observing (*in vivo*, non-invasively, and in real time) the various cross-sections beneath the observed tissue surface. Once a defect inside the S or at the tooth/S interface is identified – as in Figure 18(a) and Figure 19(e, f) – it must be corrected. Such defects left untreated/uncorrected (or even undetected, if only radiography is utilized) become sources of secondary cavities, filled (as it is well-known) with anaerobic bacteria, thus becoming a more severe dental issue than open-surface dental cavities.

Beside tooth treatments, dental crowns can and should also be investigated/verified prior to being placed in the mouth, to detect eventual inner defects (D), as those shown in Figure 18(b). Such defects are sources of cracks, that usually occur (even) within weeks after placing the crown in the patient's mouth, situation that should be avoided.

Among the sources of defects such as those in Figure 18(b) one has the loss of calibration of the dental ovens where metal ceramic or all ceramic crowns are sintered. We have studied, for the first time to our knowledge, using OCT [54, 55], this loss of calibration that produces a lower or higher than normal sintering temperature of the ceramics. OCT has thus been demonstrated to provide both qualitative [54], but, more important, quantitative results [55] in assessing the maximum temperature reached in the oven and its difference from the temperature prescribed by the manufacturer (for each specific material). Rules-of-thumb have been thus extracted in [54] from both OCT C-scans and

536 reflectivity profiles extracted from them, as well as from related parameters obtained from these
 537 profiles [55].

538 Finally, besides assessing (using OCT) performed treatments, the imaging technique can be
 539 utilized during certain dental procedures, as well. An example is presented in Figure 20, from the
 540 detailed study in [56]: OCT B-scans are retrieved during the drilling process of a dental cavity (*ex*
 541 *vivo*). Using only visual observation the dental practitioner may find difficult to avoid breaking the
 542 ceiling of the pulp chamber, while using OCT the remaining dental thickness (RDT) of this ceiling
 543 can be kept above the safety limit of approximately 0.5 mm [56]. In Figure 20 the (unwanted) situation
 544 of opening the pulp chamber is presented. In the B-scan in Figure 20(b) the moment when the fracture
 545 of the remaining dentin occurs is captured, in real time. Supervizing the drilling process with OCT
 546 may prevent the need for an endodontic undesired treatment, by mentaining the tooth integrity.



547 **Figure 20.** (a) Tooth morphology, sectioned after the procedure, showing the Remaining Dental
 548 Thickness (RDT) between the drilled cavity and the pulp chamber. An endodontic needle is inserted
 549 through the drilled cavity towards the pulp chamber, via the pulp horns, therefore the drilling process
 550 has affected the pulp chamber. (b) Real-time OCT evaluation of the RDT, showing its decrease to a
 551 critical value, for which a fracture occurs—from the detailed study in [55].
 552

553 3.5. Synergy between radiography and OCT

554 There are four aspects that differentiate radiography and OCT in terms of imaging quality:
 555 image resolution, penetration depth, field-of-view (FOV), and radiation safety. In terms of
 556 penetration depth and FOV radiography is clearly superior to OCT. In terms of resolution OCT is
 557 superior, and it is also radiation-free (while the level of radiation in a radiography imaging session,
 558 but also during all phases of a dental treatment is an issue of concern for patients, as well as
 559 professionals [8,9]). However, potentially the performance of OCT may be affected by artefacts,
 560 especially due to involuntary movements of the patient. The choice of the OCT system and of its
 561 performances must be also carefully made, to provide the necessary acquisition speed and video-
 562 frame imaging capabilities for real time, *in vivo* imaging, the latter using, for Dental Medicine,
 563 dedicated handheld probes [50-53], as demonstrated in [30, 49].

564 According to the level of details and information gathered from an image, the present study has
 565 compared OCT and radiography regarding diagnosis or treatments assessment of selected dental
 566 issues. For example, a small cavity with a width of 0.2 mm can be observed on a panoramic or on an
 567 intraoral radiography but can be correctly assessed (dimensionally) only on OCT images. The results
 568 have shown the differences in assessing a cavity and why OCT is the method of choice in the case of
 569 small cavities.

570 OCT also proves useful when details and exact measurements are needed. The drawback of OCT
 571 in this case is its limited area of investigation (given its FOV), of less than $5 \times 5 \text{ mm}^2$ (or much smaller,
 572 of $1 \times 1 \text{ mm}^2$, for example, when higher resolutions are required). In contrast, panoramic radiography
 573 covers the whole mouth. This means that it takes time to investigate all teeth with OCT, while a
 574 panoramic radiograph only takes 15 s of exposure.

575 Crown and filling adaptation are other dental aspects that are covered by both techniques. For
 576 dental fillings, OCT and 3D CBCT can be at the same level because the adaptation can be correctly

577 assessed on both 3D renderings, with a better resolution of OCT (i.e., commonly 4 to 10 μm axial
 578 resolution for OCT, and 75 to 150 μm for radiography). The drawback of radiography is the fact that
 579 when the dental crown is made of a radiopaque material such as metal, artefacts appear on images.
 580 OCT can provide accurate images of the surface of metallic objects, but it cannot penetrate the
 581 material. Therefore, when assessing the adaptation of metallic dental crowns, OCT images can offer
 582 qualitative information and details, while radiographs (both panoramic and 3D CBCT) have
 583 reconstruction artefacts because of the major amount of metal from the dental crown.

584 To summarize the results, in Table 3 one can see what type of medical imaging technique is more
 585 suitable to be utilized to diagnose or to assess the proper treatment for selected dental issues.

586 **Table 3.** Medical imaging technique suitable for selected dental issues.

Dental issue	Radiography	OCT
Cavities	Cavities smaller than 0.5 x 0.5 mm are barely visible on any type of radiography	Correct quantitative assessment of small cavities (Figures 7-10 and 15-17)
Dental crowns (metal ceramic or all ceramic)	Artefacts may appear therefore the obtained images cannot be utilized	Accurate surface images for metallic parts; high-resolution images beneath the sample surface for non-metallic (ceramic or polymer) crowns
Orthodontics	Appropriate to measure/observe teeth movement	Accurate for tooth analysis (i.e., for enamel and dentine—Figures 11, 12, and 14)
Bone issues assessment	Accurate investigations of bone density and quantity assessment on 3D CBCT images (see the example in Figure 3)	Cannot penetrate through the bone more than 1 to 2 mm
Periodontitis	The disease can be monitored during the treatment (example, Figure 5)	Exact measurements of bone loss/gain are possible
Crown/filling adaptation	High-quality images for materials that do not absorb X-ray radiation in excess	High quality images for most types of materials used in dentistry (Figure 13)
Enamel/dentine issues	Not visible on any type of radiography	Qualitative images, but also quantitative evaluations can be obtained—even beneath the teeth surface
Soft tissue	Not visible using any type of radiography	Qualitative images can be obtained. Depth limitation of up to 2 mm.

587
 588 A synergy between radiography and OCT can be concluded from the study-Table 4. First, the
 589 two methods can validate each other to some extent, as some dental issues can be investigated with
 590 both imaging techniques, including cavities, periodontitis and adaptation of dental crowns or dental
 591 fillings. Dental issues can be spotted and assessed on images gathered from both techniques, but with
 592 differences at the level of details and regarding the amount of information that can be observed on
 593 both images—as observed in the examples considered in this study.

594 **Table 4.** Medical imaging technique suitable for diagnose/treatment checking and assessment of dental
 595 issues.

Dental issue	Diagnose/Treatment monitoring	Measuring capability of their spatial extension
--------------	-------------------------------	---

Cavities	X-ray and OCT	OCT
Metal crowns	OCT	OCT
Orthodontics	X-ray and OCT	OCT
Bone assessment	X-ray	X-ray
Periodontitis	X-ray and OCT	X-ray and OCT
Crown/filling adaptation	X-ray and OCT	OCT
Enamel/dentine issues	OCT	OCT
Soft tissue	OCT	OCT

596
597
598
599
600
601

Secondly, OCT and radiography are complementary, as there are dental issues that cannot be investigated with OCT and others that cannot be investigated with radiography. Essentially, for large areas and for investigating in depth the sample, it is better to choose X-ray techniques, while for accurate high-resolution images of small area of the surface and up to 2 mm in depth of the sample, it is better to choose the OCT technique.

602 4. Conclusions

603 The study has considered various applications of Dental Medicine, comparing the performance
604 of radiography and OCT in assessing dental affections and in treatment monitoring. The reciprocal
605 validation and the complementarity of the two imaging techniques have been studied. The contrast
606 and possible synergy of radiography and OCT can be a beautiful example of Niels Bohr's principle:
607 "Contraria non contradictoria, sed complementa sunt".

608 Dental issues assessed with radiography are bone analysis, surgery monitoring (i.e., bone
609 augmentation, implant insertion), apical infections or root canal filling. OCT can be utilized when
610 there are gingiva issues, enamel or dentine problems (i.e., deformations, demineralization or cracks),
611 early stage cavities or metallic dental crowns; also, for precise measurements of dental issues (i.e.,
612 cavities, including early ones) and for monitoring dental drilling during the procedure. One must
613 also point out to other techniques that may serve to cover specific (niche) applications, including
614 Scanning Electron Microscopy (SEM) for small details in (cleaning) the apical canal, for example,
615 micro-CT (for superior resolutions than OCT-also providing 3D images) [57], as well as confocal
616 microscopy for research in dental materials, for example. However, radiography remains the
617 common technique for dentistry, while, as pointed out in the study, and considering also cost and
618 availability, OCT can become a daily-basis imaging technique in dentistry alongside radiography, as
619 well. This is also because although in this study mostly *ex vivo* OCT investigations have been
620 considered (to assess resolution and penetration capabilities), OCT imaging can be also performed *in*
621 *vivo*, as demonstrated using 1D GS- [30, 49], 2D GSs- [50, 51], and 2D MEMS-based [52, 53] handheld
622 scanning probes.

623 Advantages and drawbacks of using one technique or the other should however be considered
624 carefully for each specific application. This study may contribute to serve as a guidance in this respect.
625 Considering all aspects (i.e., image resolution/level of detail, time consuming criterion, accuracy,
626 artefacts, area of investigation/FOV, and radiation issues/invasiveness), one can thus select the most
627 suitable medical imaging technique for a certain dental issue or determine that both are needed for a
628 full clinical assessment.

629 **Author Contributions:** conceptualization, V.-F.D. and R.-A.E.; methodology, R.-A.E. and V.-F.D.; OCT system
630 development, A.P., G.D., and V.-F.D.; OCT software, A.B.; sample preparation, R.-A.E. and C.S.; X-rays
631 investigations, R.-A.E.; OCT investigations, R.-A.E., V.-F.D., and C.S.; data validation and analysis, R.-A.E. and
632 V.-F.D.; resources, V.-F.D.; writing—original draft preparation, R.-A.E. and V.-F.D.; writing—review and
633 editing, V.-F.D., A.B., G.D., and A.P.; supervision, project administration, and funding acquisition, V.-F.D. All
634 authors have read and agreed to the published version of the manuscript.

635 **Funding:** This research was funded by the Romanian National Authority for Scientific Research, CNDI-
636 UEFISCDI grant PN-III-P2-2.1-PED-2019-4423 (<http://3om-group-optomechatronics.ro/>) and by the European

637 Union through the European Regional Development Fund, the Competitiveness Operational Program, BioCell-
638 NanoART Grant POC-A1-A1.1.4-E nr. 30/2016. A.B. and A.P. acknowledge the support of the European Research
639 Council (<http://erc.europa.eu>), Grant 249889 and of the Biotechnology and Biological Sciences Research Council
640 (BBSRC) grant BB/S0166431/1 and Engineering and Physical Sciences Research Council (EPSRC) grant Rebot
641 EP/N019229/1. A.P. is also supported by the NIHR Biomedical Research Centre at Moorfields Eye Hospital NHS
642 Foundation Trust and UCL Institute of Ophthalmology, and by the Royal Society Wolfson Research Merit
643 Award.

644 **Acknowledgments:** This paper is based on a presentation prepared for the '1st International Conference –
645 *Advances in 3OM: Opto-Mechatronics, Opto-Mechanics, and Optical Metrology*', December 13-16, 2021,
646 Timisoara, Romania.

647 **Ethical approval:** For this study, several extracted teeth have been gathered from the *Dental Experts* Clinic and
648 several *in vivo* studies have been performed (the latter with the written consent of the patients), following the
649 Ethical protocol, with the Approval nr. 178/31.08.2020 of The Ethical Commission of the Clinic.

650 **Conflicts of Interest:** A. Podoleanu and A. Bradu are inventors on patents in the name of the University of Kent,
651 UK. The authors declare no other conflict of interest. The funders had no role in the design of the study; in the
652 collection, analyses, or interpretation of data; in the writing of the manuscript, or in the decision to publish the
653 results.

654 References

- 655 1. Jung, R.E.; Schneider, D.; Ganeles, J.; Wismeijer, D.; Zwahlen, M.; Hammerle, C.H.; Tahmeseb,
656 A. Computer Technology Applications in Surgical Implant Dentistry: A Systematic Review. *The*
657 *International J. of Oral & Maxillofacial Implants* **2009**, *24*, 92-109.
- 658 2. Lin, L.; Fang, Y.; Liao, Y.; Chen, G.; Gao, C.; Zhu, O. 3D Printing and Digital Processing
659 Techniques in Dentistry: A Review of Literature. *Advanced Engineering Materials* **2019**, *21*(6).
- 660 3. Javaid, M.; Haleem, A.; Kumar, L. Current status and applications of 3D scanning in dentistry.
661 *Clinical Epidemiology and Global Health* **2019**, *7*(2), 228-233.
- 662 4. Huang, D.; Swanson, E.A.; Lin, C.P.; Schuman, J.S.; Stinson, W.G.; Chang, W.; Hee, M.R.; Flotte,
663 T.; Gregory, K.; Puliafito, C.A.; Fujimoto, J.G. Optical coherence tomography. *Science* **1991**, *254*,
664 1178-1181.
- 665 5. Choma, M.A.; Sarunic, M.V.; Yang, C.; Izatt, J.A. Sensitivity advantage of swept-source and
666 Fourier-domain optical coherence tomography. *Opt. Express* **2003**, *11*, 2183-2189.
- 667 6. Drexler, W.; Liu, M.; Kumar, A.; Kamali, T.; Unterhuber, A.; Leitgeb, R.A. Optical coherence
668 tomography today: speed, contrast, and multimodality. *J. Biomed. Opt.* **2014**, *19*, 071412.
- 669 7. Podoleanu, A.; Bradu, A. Master-slave interferometry for parallel spectral domain
670 interferometry sensing and versatile 3D optical coherence tomography. *Opt. Express* **2013**, *21*,
671 19324–19338.
- 672 8. Poppe, B.; Looe, H.K.; Pfaffenberger, A.; Chofor, N.; Eenboom, F.; Sering, M.; Rühmann, A.;
673 Poplawski, A.; Willborn, K. Dose-area product measurements in panoramic dental radiology.
674 *Radiation Protection Dosimetry* **2007** *123*(1), 131-134.
- 675 9. Erdelyi, R.A.; Duma, V.-F. Optimization of radiation doses and patients' risk in dental
676 radiography. *AIP Proceedings* **2019** *2071*, 040013.
- 677 10. Feldchtein, F.; Gelikonov, V.; Iksanov, R.; Gelikonov, G.; Kuranov, R.; Sergeev, A.; Gladkova, N.;
678 Ourutina, M.; Reitze, D.; Warren, J. *In vivo* OCT imaging of hard and soft tissue of the oral cavity.
679 *Opt. Express* **1998** *3*, 239-250.
- 680 11. Otis, L.; Everett, M.J.; Sathyam, U.S.; Colston Jr., B.W. Optical Coherence Tomography: A New
681 Imaging: Technology for Dentistry. *The J. of the American Dental Association* **2000**, *131*(4), 511-514.
- 682 12. Monteiro G Queiroz de Melo, Montesa, M.A.J.R.; Gomes, A.S.L.; Motac, C.B.O.; Sérgio, L.;
683 Freitas, A.Z. Marginal analysis of resin composite restorative systems using optical coherence
684 tomography. *Dent. Mat.* **2011**, *27*, 213–223.
- 685 13. Nakagawa, H.; Sadr, A.; Shimada, Y.; Tagami, J.; Sumi, Y. Validation of swept source optical
686 coherence tomography (SS-OCT) for the diagnosis of smooth surface caries *in vitro*. *J. Dent.* **2013**,
687 *41*, 80-89.

- 688 14. Hsieh, Y.-S.; Ho, Y.-C.; Lee, S.-Y.; Chuang, C.-C.; Tsai, J.; Lin, K.-F.; Sun, C.-W. Dental Optical
689 Coherence Tomography. *Sensors* **2013** *13*, 8928-8949.
- 690 15. Schneider, H.; Park, K.-J., Häfer, M., Rüger, C., Schmalz, G., Krause, F., Schmidt, J., Ziebolz, D.,
691 Haak, R. Dental Applications of Optical Coherence Tomography (OCT) in Cariology. *Appl. Sc.*
692 **2017**, *7*, 472.
- 693 16. Yang, V.; Curtis, D.A.; Fried, D. Use of Optical Clearing Agents for Imaging Root Surfaces with
694 Optical Coherence Tomography. *IEEE J. of Selected Topics in Quantum Electronics* **2019**, *25*,
695 7100507.
- 696 17. Erdelyi, R.A.; Duma, V.-F.; Dobre, G.; Bradu, A.; Podoleanu, A. A combination of imaging
697 techniques for dental medicine: from x-rays radiography and 3D CBCT to OCT. *Proc. SPIE* **2020**,
698 11359, 113591E.
- 699 18. Drexler, W.; Fujimoto, J.G., Eds. *Optical Coherence Tomography: Technology and Applications*.
700 Springer International Publishing: Switzerland, 2015.
- 701 19. Lee, K.-S.; Zhao, H.; Ibrahim, S.F.; Meemon, N.; Khoudeir, L.; Rolland, J.P. Three-dimensional
702 imaging of normal skin and nonmelanoma skin cancer with cellular resolution using Gabor
703 domain optical coherence microscopy. *J. Biomed. Opt.* **2012**, *17*(12), 126006.
- 704 20. Adler, D.C.; Chen, Y.; Huber, R.; Schmitt, J.; Connolly, J.; Fujimoto, J.G. Three-dimensional
705 endomicroscopy using optical coherence tomography. *Nature Photonics* **2007**, *1*, 709–716.
- 706 21. Choi, W.J.; Wang, R.K. In vivo imaging of functional microvasculature within tissue beds of oral
707 and nasal cavities by swept-source optical coherence tomography with a forward/side-viewing
708 probe. *Biomed. Opt. Express* **2014**, *5*, 2620-2634.
- 709 22. Canavesi, C.; Rolland, J.P. Ten Years of Gabor-Domain Optical Coherence Microscopy, *Appl. Sc.*
710 **2019**, *9*(12), 2565.
- 711 23. Povazay, B.; Bizheva, K.; Unterhuber, A.; Hermann, B.; Sattmann, H.; Fercher, A.F.; Drexler, W.;
712 Apolonski, A.; Wadsworth, W.J.; Knight, J.C.; Russell, P.St.J.; Vetterlein, M.; Scherzer, E.
713 Submicrometer axial resolution optical coherence tomography. *Opt. Lett.* **2002**, *27*, 1800-1802.
- 714 24. Lehmann, T.M.; Troeltsch, E.; Spitzer K. Image processing and enhancement provided by
715 commercial dental software programs. *Dentomaxillofacial Radiology* **2002** *31*, 264-272.
- 716 25. Imaging Manual, “en 3D s/Classic with ProTouch”, 21.05.2019,
717 <https://materialbank.planmeca.com/> (accessed on 20.09.2019).
- 718 26. Yeung, A.W.K.; Jacobs, R.; Bornstein, M.M. Novel low-dose protocols using cone beam
719 computed tomography in dental medicine: a review focusing on indications, limitations, and
720 future possibilities. *Clin. Oral Invest.* **2019** *23*, 2573–2581.
- 721 27. Versteeg, C.H.; Sanderink, G.C.H. van der Stelt, P.F. Efficacy of digital intra-oral radiography in
722 clinical dentistry. *J. of Dentistry* **1997** *25*(3–4), 215-224.
- 723 28. Erdelyi, R.A.; Duma, V.-F.; Dobre, G.; Bradu, A.; Podoleanu, A. Investigations of dental cavities:
724 between X-ray radiography and OCT. *Proc. SPIE* **2019** *11385*, 1138504.
- 725 29. Duma, V.-F. Laser scanners with oscillatory elements: Design and optimization of 1D and 2D
726 scanning functions. *Applied Mathematical Modelling* **2019** *67*(3), 456-476.
- 727 30. Duma, V.-F.; Dobre, G.; Demian, D.; Cernat, R.; Sinescu, C.; Topala, F.I.; Negrutiu, M.L.; Hutiu,
728 Gh.; Bradu, A.; Podoleanu, A.Gh. Handheld scanning probes for optical coherence tomography.
729 *Romanian Reports in Physics* **2015** *67*(4), 1346-1358.
- 730 31. Oancea, R.; Bradu, A.; Sinescu, C.; Negru, R.M.; Negrutiu, M.L.; Antoniac, I.; Duma, V.-F.;
731 Podoleanu, A.Gh. Assessment of the sealant/tooth interface using optical coherence
732 tomography. *J. of Adhesion Science and Technology* **2015**, *29*(1), 49-58.
- 733 32. Romexis Viewer user’s manual, <http://www.planmecausa.com> (25.09.2019).
- 734 33. Carranza, F.A. Carranza’s Clinical Periodontology, 10th Edition, Edited by Cochrane DL,
735 Giannobile WV, Kenney E.B., Novak M.J. St. Louis, Elsevier **2007**.
- 736 34. Gomes-Filho, I.S.; Sarmiento, V.A.; De Castro, M.S. Radiographic features of periodontal bone
737 defects: evaluation of digitized images. *Dentomaxillofac. Radiol.* **2007** *36*, 256.
- 738 35. Misch, K.A.; Yi, E.S.; Sarmient, D.P. Accuracy of cone beam computed tomography for
739 periodontal defect measurements. *J. of Periodontology* **2006** *77*, 1261.

- 740 36. Velea, O.A.; Sinescu, C.; Zeicu, C.; Freiman, P.C.; Velea, P.I.; Onisei, D.; Duma, V.-F. Evaluation
741 of Periodontal Pockets using Different Biomaterials. *Revista de Chimie* **2014**, *65*(9).
- 742 37. Sinescu, C.; Negrutiu, M.L.; Manole, M.; de Sabata, A.; Rusu, L.-C.; Stratul, S.; Dudea, D.; Dughir,
743 C.; Duma V.-F. Retractions of the gingival margins evaluated by holographic methods. *Proc.*
744 *SPIE* **2015**, *9508*, 95080V.
- 745 38. Bellucci, D.; Cannillo, V.; Sola, A. Shell Scaffolds: A new approach towards high strength
746 bioceramic scaffolds for bone regeneration, *Materials Letters* **2010**, *64*, 203–206.
- 747 39. Deb, P.; Deoghare, A.B.; Borah, A.; Barua, E.; Das Lala, S. Scaffold Development Using
748 Biomaterials: A Review. *Materials Today: Proceedings* **2018**, *5*, 12909–12919.
- 749 40. Shahgholia, M.; Olivierod, S.; Bainob, F.; Vitale-Brovaroneb, C.; Gastaldia, D.; Venaa, P.
750 Mechanical characterization of glass-ceramic scaffolds at multiple characteristic lengths through
751 nanoindentation. *J. of the European Ceramic Society* **2016**, *36*, 2403–2409.
- 752 41. Luca, R.; Todea, C.D.; Duma, V.-F.; Bradu, A.; Podoleanu, A. Quantitative assessment of rat bone
753 regeneration using complex master–slave optical coherence tomography, *Quantitative Imaging in*
754 *Medicine and Surgery* **2019**, *9*(5), 782-798.
- 755 42. Luca, R.E.; Giuliani, A.; Mănescu, A.; Heredea, R.; Hoinoiu, B.; Constantin, G.D.; Duma, V.-F.;
756 Todea, C.D. Osteogenic Potential of Bovine Bone Graft in Combination with Laser
757 Photobiomodulation: An Ex Vivo Demonstrative Study in Wistar Rats by Cross-Linked Studies
758 Based on Synchrotron Microtomography and Histology, *Int. J. of Molecular Sc.* **2020**, *21*(3), 778.
- 759 43. Duma, V.-F.; Tankam, P.; Huang, J.; Won, J.J.; Rolland, J.P. Optimization of galvanometer
760 scanning for Optical Coherence Tomography. *Appl. Opt.* **2015**, *54*, 5495-5507.
- 761 44. Alshahni, R. Z.; Shimada, Y.; Zhou, Y.; Yoshiyama, M.; Sadr, A.; Sumi Y.; Tagami, J. Cavity
762 adaptation of composite restorations prepared at crown and root: Optical assessment using SS-
763 OCT. *Dent. Mat.* **2019**.
- 764 45. Ko, A.C.-T.; Choo-Smith, L.-P.; Hewko, M.D.; Leonardi, L.; Sowa, M.G.; Dong, C.C.C.S.;
765 Williams, P.; Cleghorn, B. Ex vivo detection and characterization of early dental caries by optical
766 coherence tomography and Raman spectroscopy. *J. of Biomed. Opt.* **2005**, *10*(3), 031118.
- 767 46. Amaechi, B.T.; Higham, S.M.; Podoleanu, A.G.; Rogers, J.A.; Jackson, D.A. Use of optical
768 coherence tomography for assessment of dental caries: quantitative procedure. *J. of Oral*
769 *Rehabilitation* **2001**, *28*(12), 1092-1093.
- 770 47. Canjau, S.; Todea, C.; Negrutiu, M.L.; Sinescu, C.; Topala, F.I.; Marcautuanu, C.; Manescu, A.;
771 Duma, V.-F.; Bradu, A.; Podoleanu, A. Optical Coherence Tomography for Non-Invasive ex vivo
772 Investigations in Dental Medicine - a Joint Group Experience (Review). *Modern Technologies in*
773 *Medicine* **2015**, *7*(1), 97–115.
- 774 48. de Boer, J.F.; Hitzengerger, C.K.; Yasuno, Y. Polarization sensitive optical coherence tomography
775 – a review [Invited]. *Biomed. Opt. Express* **2017**, *8*, 1838-1873.
- 776 49. Demian, D.; Duma, V.-F.; Sinescu, C.; Negrutiu, M.L.; Cernat, R.; Topala, F.I.; Hutiu, Gh.; Bradu,
777 A.; Podoleanu, A.Gh. Design and testing of prototype handheld scanning probes for optical
778 coherence tomography. *J. of Eng. in Medicine* **2014**, *228*(8), 743-753.
- 779 50. Jung, W.; Kim, J.; Jeon, M.; Chaney, E.J.; Stewart, C.N.; Boppart, S.A. Handheld optical coherence
780 tomography scanner for primary care diagnostics. *IEEE Trans. on Biomed. Eng.* **2011**, *58*, 741-744.
- 781 51. Monroy, G.L.; Won, J.; Spillman, D.R.; Dsouza, R.; Boppart, St.A. Clinical translation of handheld
782 optical coherence tomography: practical considerations and recent advancements. *J. Biomed. Opt.*
783 **2017**, *22*(12), 121715.
- 784 52. Lu, C.D.; Kraus, M.F.; Potsaid, B.; Liu, J.J.; Choi, W.; Jayaraman, V.; Cable, A.E.; Hornegger, J.;
785 Duke, J.S.; Fujimoto, J.G. Handheld ultrahigh speed swept source optical coherence tomography
786 instrument using a MEMS scanning mirror. *Biomed. Opt. Express* **2014**, *5*, 293-311.
- 787 53. Cogliati, A.; Canavesi, C.; Hayes, A.; Tankam, P.; Duma, V.-F.; Santhanam, A.; Thompson, K.P.;
788 Rolland, J.P. MEMS-based handheld scanning probe for distortion-free images in Gabor-Domain
789 Optical Coherence Microscopy. *Opt. Express* **2016**, *24*(12), 13365-13374.

- 790 54. Sinescu, C.; Bradu, A.; Duma, V.-F.; Topala, F.; Negrutiu, M.L.; Podoleanu, A. Effects of the
791 temperature variations in the technology of metal ceramic dental prostheses: Non-destructive
792 detection using optical coherence tomography. *Appl. Sc.* **2017**, *7*, 552.
- 793 55. Duma, V.-F.; Sinescu, C.; Bradu, A.; Podoleanu, A. Optical Coherence Tomography
794 Investigations and Modeling of the Sintering of Ceramic Crowns. *Materials* **2019**, *12*(6), 947.
- 795 56. Sinescu, C.; Negrutiu, M.L.; Bradu, A.; Duma, V.-F.; Podoleanu, A.Gh. Noninvasive quantitative
796 evaluation of the dentin layer during dental procedures using Optical Coherence Tomography.
797 *Computational and Mathematical Methods in Medicine* **2015**, Paper ID 709076.
- 798 57. Zaharia, C.; Duma, V.-F.; Sinescu, C.; Socoliuc, V.; Craciunescu, I.; Turcu, R.P.; Marin, C.N.;
799 Tudor, A.; Rominu, M.; Negrutiu, M.-L. Dental adhesive interfaces reinforced with magnetic
800 nanoparticles: Evaluation and modeling with micro-CT versus optical microscopy. *Materials*
801 **2020**, *13*(9), 3908.



© 2020 by the authors. Submitted for possible open access publication under the terms and conditions of the Creative Commons Attribution (CC BY) license (<http://creativecommons.org/licenses/by/4.0/>).

802